# Sensorless Speed Control of Induction Motor for Photovoltaic Pumping System

Hamza Bouzeria[#1], Cherif Fetha[#2], Tahar Bahi[*3], Zakaria Layate[*4], Salima Lekhchine[**5]

[#]*Electrical Engineering Department, LEB Laboratory, Hadj Lakhdar University*
*Batna 05000, Algeria*
[1]bhamza23000@gmail.com
[2]cheriffetha@gmail.com

[*] *Electrical Engineering Department, Badji Mokhtar University*
*PBox 12, Annaba, Algeria*
[3]tbahi@hotmail.fr
[4]zakarialayate@gmail.com

[**] *Department of Electrical Engineering, 20 August 1955 University*

*Skikda 21000, Algeria*
[5]slekhchine@yahoo.fr

*Abstract*— **In this paper, we presents an implementation and design of intelligent speed controller of photovoltaic pumping system drive by induction motor. The fuzzy logic controller is used in indirect vector control scheme, where induction motor is fed by photovoltaic generator. Thus, the study system in our paper consists of a photovoltaic generator associated with the boost converter controlled by the technique of fuzzy logic to provide maximum power point. Moreover, adaptation of the rotor time constant powered by a photovoltaic solar energy, the latter control system adopts inverter current control scheme with variable hysteresis band. The topology control and simulation results with Matlab / Simulink according the speed and torque variations are presented and interpreted.**

*Keywords*— **Photovoltaic Pump; Induction Motor; Fuzzy logic controller; MPPT; Simulink**

## I. INTRODUCTION

In the natural, there are many field and forms of renewable energy, then the most commonly used are: solar, wind, water, biomass and geothermal energy. A great part of the energy from the sun is in the form of heat that is transmitted by infrared radiation, this exhibits the effect of photovoltaic (PV). The standalone photovoltaic water pumping systems (PVWPS) is one of the most important applications in PV systems, it have become a favourable solution for water supply, gaining more acceptance and market share, particularly in rural: areas that have a substantial amount of insolation and have no access to an electric network. So, the photovoltaic pumping systems are used to pump water for livestock, plants or humans. Since the need for water is greatest on hot sunny days, the technology is an obvious choice for this application. Agricultural watering needs are usually greatest during sunnier periods when more water can be pumped with a solar system. PV powered pumping systems are excellent for small to medium scale pumping and there are thousands of agricultural PV water pumping systems in the field today throughout the world [1-2].

In the some countries like south of Algeria has one of the fastest growing solar surface in this continent. However, it's remotely isolated rural areas posed problems to rural energy management and development of PV energy sources. The average annual daily solar radiation is within the range of 5000 – 7000 Wh/m²/day [3].

The major problem of Photovoltaic Generator (PVG) is their characteristic non-linear, and its optimum operating point depends on climatic conditions such as the temperature, the solar radiation and also the load variations. Indeed, an effective solution must ensure that the PVG runs at the maximum power point (MPP) and that the motor runs at a high efficiency level.

The objective to control the DC-DC converter type boost is the one hand by acting on the duty cycle (d) using by MPPT based on fuzzy logic controller (FLC) and the inverter on the other control by using the vector mode by FLC direction of rotor flux in order to control the torque and speed. Thus, we check the robustness of the control strategy is insensitive to the motor parameters variations [4]. In this work, we proposed an efficient speed controller scheme that can achieve high accuracy and a fast dynamic response of the electrical machine. We present an online fuzzy optimization of the global efficiency of a PVWPS driven by IM were introduced mainly for their robustness and relatively low cost [5], coupled to a centrifugal pump. Water discharge is depends on opening valve and the speed of the motor, the speed can be controlled by frequency supplied by the inverter to the motor.

The fuzzy optimization procedure, which aims to the maximization of the global efficiency, has led consequently to maximize the drive speed and the water discharge rate of the coupled centrifugal pump using with variable rotational speed and modular number of working stages, thus achieving the highest efficiency of the system for all conditions [6].

The paper is organized as follows: in section II the proposed and study system is presented. Section III we illustrate the design of fuzzy logic methodology. In section IV, flux and speed estimate is developed. Section discuss for indirect vector control. Finally, section V presents the simulation and results obtained with the proposed techniques.

## II. SYSTEM STUDY

The study system of photovoltaic water pump is shown in Fig. 1. Where is consists for PVG, power converters, IM, pump and controllers blocks.
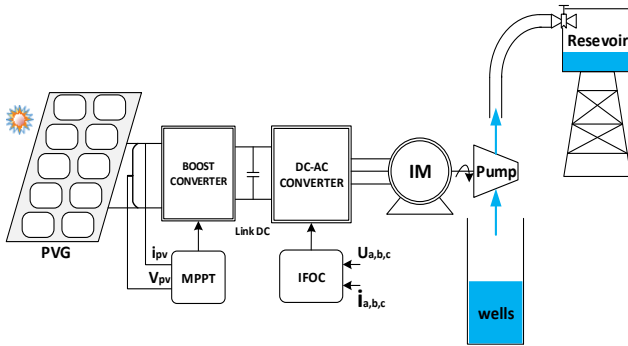


Fig. 1 Photovoltaic pumping system scheme

### A. Model of Photovoltaic Generator

The direct conversion of the solar energy into electrical power is obtained by solar cells. Solar cells as they are often called are semiconductor devices that convert sunlight into direct current electricity. Groups of PV cells are electrically configured into modules and arrays. The solar cell may be modelled by a current source in parallel with a diode, so shunt and a series resistance are added to the model. The equivalent circuit of solar cell is shown in Fig. 2.
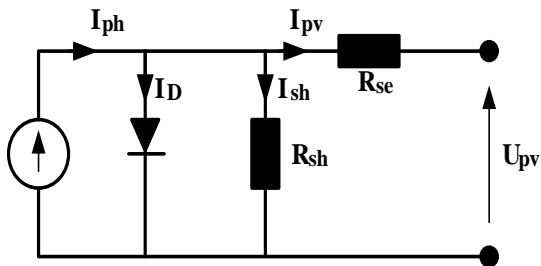


Fig. 2 Equivalent circuit of photovoltaic panel

The PV panel is composed of $N_P$ parallel modules. Each one including $N_S$ photovoltaic cell serial connected. The fundamental equation for PV model is given by (1) [7]:

$$I_{pv} = N_p I_{ph} - N_p I_0 \left\{ \exp\left[\frac{q(U_{pv}+I_{pv}R_{se})}{akTN_s}\right] - 1 \right\} - \frac{U_{pv}+I_{pv}R_{se}}{R_{sh}} \qquad (1)$$

$$I_0 = I_{or} \left(\frac{T}{T_r}\right)^3 \exp\left\{\frac{qE_G}{ka}\left[\frac{1}{T_r} - \frac{1}{T}\right]\right\} \qquad (2)$$

$$I_{ph} = \{I_{sc} + k_i(T - 298)\}\frac{G}{G_n} \qquad (3)$$

where,

| | |
|---|---|
| $I_{pv}$ | : PV panel output current |
| $U_{pv}$ | : V panel output voltage |
| $I_{ph}$ | : generated photocurrent |
| $R_{sh}, R_s$ | : parallel and series resistance, respectively |
| Q | : electron charge |
| K | : Boltzmann's constant |
| A | : p–n junction ideality factor |
| $I_0, I_{0r}$ | : real and reference cell reverse saturation current, respectively |
| $k_i$ | : temperature coefficient for short circuit current |
| $T, T_r$ | : real and reference temperature, respectively |
| $I_{sc}$ | : short-circuit current |
| $G, G_n$ | : solar radiation and nominal radiation, respectively |

### B. Power Converters Model

Due to the variation of climatic conditions, the PV module provides power to the load via a regulated converter to maintain maximum power. The chopper amplifier circuit considered is shown in Fig. 3.
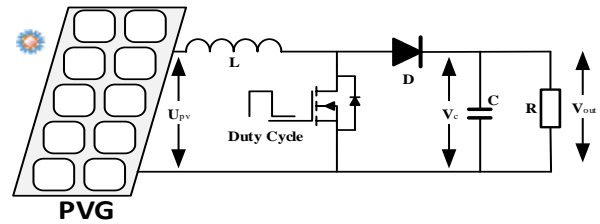


Fig. 3 Boost converter model

The output voltage of the DC converter can be expressed by the following equation [8]:

$$V_{out} = V_c = \frac{V_{pv}}{1-D} \qquad (4)$$

The voltage $V_{out}$ is applied to the inverter input terminals of two capacitors $C_1$ and $C_2$ used to create the midpoint fictitious. The Voltage arms at the midpoint of the DC bus is expressed by the following equations [9]:

$$\begin{cases} V_{io} = +\frac{V_{out}}{2} \text{ if } S_i = 1 \text{ avec } (i = 1,2,3) \\ V_{io} = -\frac{V_{out}}{2} \text{ if } S_i = 1 \text{ avec } (i = 4,5,6) \end{cases} \qquad (5)$$

And, the phase voltages at the terminals of the load are:

$$\begin{cases} U_{An} = \frac{2}{3}U_{A0} - \frac{1}{3}U_{B0} - \frac{1}{3}U_{C0} \\ U_{Bn} = -\frac{1}{3}U_{A0} + \frac{2}{3}U_{B0} - \frac{1}{3}U_{C0} \\ U_{Cn} = -\frac{1}{3}U_{A0} - \frac{1}{3}U_{B0} + \frac{2}{3}U_{C0} \end{cases} \qquad (6)$$

With,

$$U_n = \frac{1}{3}(U_{A0} + U_{B0} + U_{C0}) \tag{7}$$

### C. Induction Motor Model

The mathematical model of the induction motor in the synchronous reference may be in the form of the following state equation [10]:

$$\begin{cases} \frac{di_{ds}}{dt} = \frac{1}{\sigma L_s}\left[-R_{sr}i_{ds} + \omega_s\sigma L_s i_{qs} + \frac{L_m R_r}{L_r^2}\Phi_{dr} + \frac{L_m}{L_r}\omega_r\Phi_{qr} + v_{ds}\right] \\ \frac{di_{qs}}{dt} = \frac{1}{\sigma L_s}\left[-R_{sr}i_{qs} - \omega_s\sigma L_s i_{ds} + \frac{MR_r}{L_r^2}\Phi_{qr} + \frac{L_m}{L_r}\omega_r\Phi_{dr} + v_{qs}\right] \\ \frac{d\Phi_{dr}}{dt} = \frac{L_m R_r}{L_s}i_{ds} - \frac{R_r}{L_r}\Phi_{dr} + \omega_g\Phi_{qr} \\ \frac{d\Phi_{qr}}{dt} = \frac{L_m R_r}{L_s}i_{qs} - \frac{R_r}{L_r}\Phi_{qr} + \omega_g\Phi_{dr} \end{cases} \tag{8}$$

$$T_e = n_p \frac{L_m}{L_r}\left(\Phi_{dr}i_{qs} - \Phi_{qr}i_{ds}\right) \tag{9}$$

$$J\frac{d\omega_r}{dt} + f\omega_r = T_e - T_L \tag{10}$$

where, $\omega_g = \omega_s - \omega_r$, $R_{sr} = \left(R_s + R_r\frac{L_m^2}{L_r^2}\right)$ and $\sigma = \left(1 - \frac{L_m^2}{L_s L_r}\right)$

$\Phi$: the flux linkage; L: the inductance; v: the voltage; R: the resistance; i: the current; $\sigma$: the motor leakage coefficient. $\omega_r$: the rotor electrical speed. The subscripts "r" and "s" are the rotor and stator values respectively refereed to the stator, and the subscripts "d and "q denote the d-q axis components in the stationary reference frame. However, in the case of a supply voltage $v_{ds}$ and $v_{qs}$ influence on both ids and $i_{qs}$, so the flux and torque, which is the value of adding compensation terms to make d and q axes are completely independent. The performance brings the additional decoupling also told by compensation were shown in [11].

### D. Centrifugal Pump Model

The centrifugal pump model illustrate by (11), presents a model based on motor dynamics. Effects of pump flow rate and speed are shown in modelling equation. The equation is a form of Riccatti equation where a, b and c are determinable constants from pump geometry.

$$H_p = xQ^2 + yQN + zN^2 \tag{11}$$

This equation shows the influence of flow rate and speed on outlet pressure of the centrifugal pump; also it can match with steady - state conditions of pressure versus flow rate curve. The pump torque in a form of similar function of flow rate and speed may be modelled like as (12) [12].

$$T_p = uQ^2 + vQN + wN^2 \tag{12}$$

Frictional torque as a function of friction coefficient and rotational speed may be added to pump torque in order to form the load torque according to (13).

$$T_l = T_p + T_{friction} = T_p + B.N \tag{13}$$

Equations (11) to (13) together form the centrifugal pump model which the flow rate from the consumption network and the rotational speed from the induction motor are its inputs where the head to the consumption network and the load torque to the induction motor.

### III. FUZZY LOGIC CONTROL

The artificial intelligent for maximum power point technique is fast uses for robustness system, so, this power can be delivered by a PVG depends greatly on variation of climatic conditions. Therefore, it is necessary to track the MPP all the time. They have the advantage to be robust and relatively simple to design as they do not require the knowledge of the exact model. They do require on the other hand the complete knowledge of the operation of the PV system.
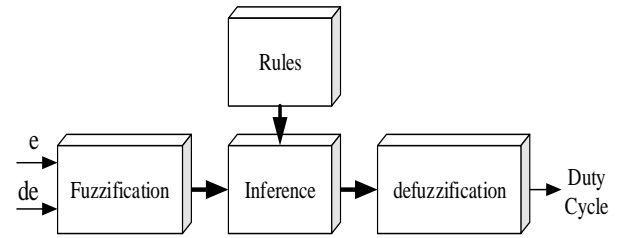


Fig. 4 Fuzzy logic control design

The FLC input variables are the error (e) and derivate of error (de) at sampled times k defined by [13]:

$$\begin{cases} e(k) = \frac{P_{pv}(k) - P_{pv}(k-1)}{V_{pv}(k) - V_{pv}(k-1)} \\ de(k) = e(k) - e(k-1) \end{cases} \tag{14}$$

The FLC tracks the MPP based on master rule of "If X and Y, Then Z" [14]. To determine the output of the positive, negative and zero sequence voltages, currents, and impedances fuzzy logic, the inference is used. There are many methods for inference but the popular one is Memdani. Other methods include compositional rule of inference, generalized modus ponens and Sugeno inference method. The fuzzy inference is carried out by using Mamdani's method and the defuzzification uses the centre of gravity to compute the output of this FLC which is the optimum duty cycle. The control rules are indicated in Table I.

TABLE I
FUZZY RULES

| de\e | NB | NM | NS | ZE | PS | PM | PB |
|------|----|----|----|----|----|----|----|
| NB | NB | NB | NB | NB | NM | NS | ZE |
| NM | NB | NB | NB | NM | NS | ZE | PS |
| NS | NB | NB | NM | NS | ZE | PS | PM |
| ZE | NB | NM | NS | ZE | PS | PM | PB |
| PS | NM | NS | ZE | PS | PM | PB | PB |
| PM | NS | ZE | PS | PM | PB | PB | PB |
| PB | ZE | PS | PM | PB | PB | PB | PB |

## IV. FLUX AND SPEED ESTIMATION

Many schemes based on simplified motor models have been devised to sense the speed of the induction motor from measured terminal quantities for control purposes. In order to obtain an accurate dynamic representation of the motor speed, it is necessary to base the calculation on the coupled circuit equations of the motor. However, the performance of these methods is deteriorated at a low speed because of the increment of nonlinear characteristic of the system. The current paper proposes a new rotor speed estimation method to improve the performance of a sensorless vector controller in the low speed region and at zero speed. From the stator voltage equations in the stationary frame it is obtained [15]:

$$\begin{cases} \frac{d\Phi_{dr}}{dt} = \frac{L_r}{L_m}\left(v_{ds} - R_s i_{ds} - \sigma L_s \frac{di_{ds}}{dt}\right) \\ \frac{d\Phi_{qr}}{dt} = \frac{L_r}{L_m}\left(v_{qs} - R_s i_{qs} - \sigma L_s \frac{di_{qs}}{dt}\right) \end{cases} \quad (15)$$

Using the rotor flux and motor speed, the stator current is represented as:

$$\begin{cases} i_{ds} = \frac{1}{L_m}\left(\Phi_{dr} + \omega_r T_r \Phi_{qr} - T_r \frac{d\Phi_{dr}}{dt}\right) \\ i_{qs} = \frac{1}{L_m}\left(\Phi_{qr} - \omega_r T_r \Phi_{dr} - T_r \frac{d\Phi_{qr}}{dt}\right) \end{cases} \quad (16)$$

where, $T_r = L_r/R_r$ is the rotor time constant.

From the equations (15) and (16) and using the estimated speed, the stator current is estimated as:

$$\begin{cases} i_{ds}^e = \frac{1}{L_m}\left(\Phi_{dr} + \omega_r^e T_r \Phi_{qr} - T_r \frac{d\Phi_{dr}}{dt}\right) \\ i_{qs}^e = \frac{1}{L_m}\left(\Phi_{qr} - \omega_r^e T_r \Phi_{dr} - T_r \frac{d\Phi_{qr}}{dt}\right) \end{cases} \quad (17)$$

Where, $i_{ds}^e$ and $i_{qs}^e$ are the estimated stator currents and $\omega_{re}$ is the estimated rotor electrical speed. The vector control rotor flux oriented is called direct or indirect method to estimate the rotor flux vector.

## V. ADAPTIVE CURRENT HYSTERESIS BAND CONTROL

The adaptive hysteresis band is used to control load currents and determine switching signals for semiconductor gates. Suitable stability, fast response, high accuracy, simple operation, inherent current peak limitation and load parameters variation independency make the current control methods of voltage source inverters.
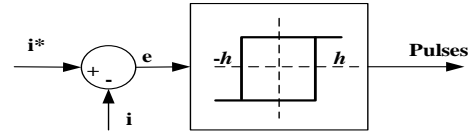


Fig. 5  Principal of hysteresis current control

In this approach the current error is a difference between the reference current and the recent current injected by the inverter err(t)= $I_{ref}(t)$ - I (t). When the error current exceeds the upper limit of the hysteresis band, the upper switch of the inverter arm is turned to zero Boolean "0" and the lower switch is turned to one Boolean "1". When the error current crosses the lower limit of the hysteresis band (HB), the lower switch of the inverter arm is turned "0" and the upper switch is turned "1"[16]. As a result, the current gets back into the hysteresis band. The switching performance as follows:

$$K = \begin{cases} 0 & \text{if } i_{Inv}(t) > i_{ref}(t) + HB \\ 1 & \text{if } i_{Inv}(t) < i_{ref}(t) - HB \end{cases} \quad (18)$$
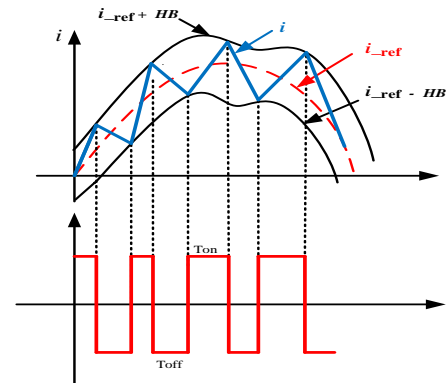


Fig. 6  Structure of hysteresis current control
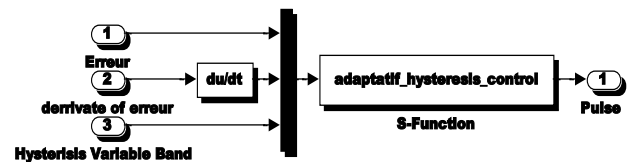


Fig. 7  Simulink bloc of hysteresis current control

Fig. 8  Hysteresis current control

$$\Phi_{dr}^e = \frac{R_s L_m}{R_r + L_r P} i_{ds}^e \tag{22}$$

$$\omega_{sl}^e = \omega_s - \omega_r = \frac{R_r i_{ds}^e}{L_r i_{ds}^e} \tag{23}$$
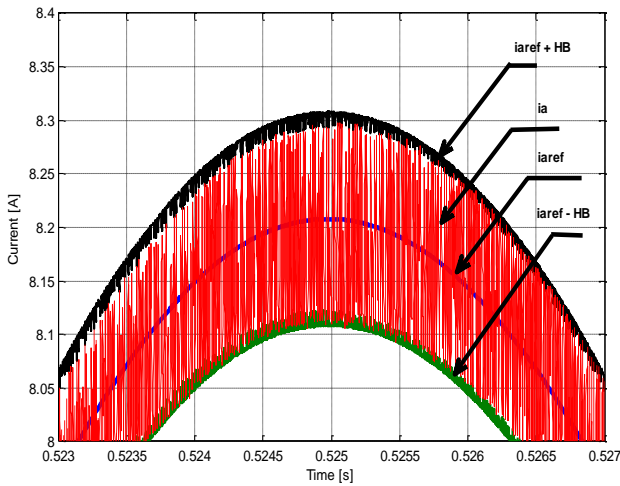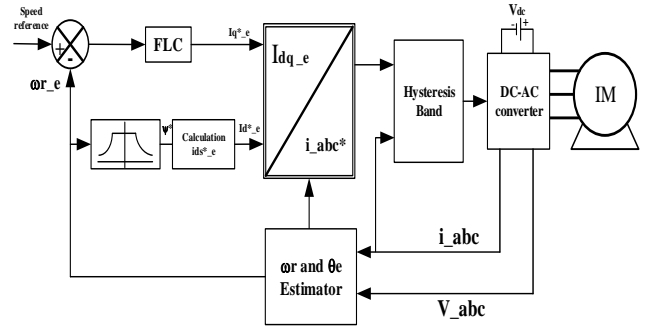


Fig. 9  Block diagram of IFOC scheme based IM drive

## VI. INDIRECT FIELD ORIENTED VECTOR CONTROL

The diagram block of IFOC for IM is shown in Fig. 9. It consists of two feedback control loops. The inner loop is a conventional synchronous current regulation loop. The torque command current, $i_{qs}^*$, is produced by selected controller in the outer speed loop, based on the command speed $\omega_r^*$ and the actual speed $\omega_r$ [17]. The success of FOC is based on the proper division of stator current into two components: the torque component $i_{qs}^*$ and magnetizing flux component $i_{ds}^*$. The indirect FOC method uses a slip equation for partitioning the stator current.

$$\omega_r^* = \frac{R_r i_{qs}^{e*}}{L_r i_{ds}^{e*}} \tag{19}$$

The axis are fixed on the stator, but the $d_r$-$q_r$ axes, which are fixed on the rotor , are $d_s$-$q_s$ moving at speed $\omega_r$ synchronously rotating axes $d_e$-$q_e$ are rotating ahead of the $d_r$-$q_r$ axes by the positive slip angle $\theta_s$ corresponding to slip frequency $\omega_{sl}$. Since the rotor pole is directed on the de axes and $\omega_e = \omega_r + \omega_{sl}$ one can write:

$$\theta_e = \int \omega_e dt = \int (\omega_r + \omega_{sl}) dt = \theta_r + \theta_{sl} \tag{20}$$

The phase diagram suggests that for decoupling control, the stator flux component of current $i_{ds\_e}$ should be aligned on the de axis and the torque component of current $i_{qs\_e}$ should be $\theta$ the $q_e$ axis, as shown. For decoupling control, one can make a derivation of control equations of IFOC with the help of $d_e$-$q_e$ dynamic model of IM .one can easily show the following important equations:

$$T_e = \frac{3PL_m}{4L_r} \left( \Phi_{dr}^e i_{qs}^e \right) \tag{21}$$

## VII. SIMULATION RESULTS

The different parts are programmed to bases of their respective models and mainly two types of controllers are tested and their results analyzed.

The simulation results are shown in Fig. 10 and 11 respectively. The state of change in the 0.3s and 0.6s between valve affects the pump so that the flow rate and pressure as shown in Fig. 10. In other words, the influence on the motor results in the variation of torque and speed, so that the fuzzy logic control regulates the drives according to maintain constant the desired set point. Regarding Fig. 11, we note that the rate stabilizes at its value at 0.12 s and remains constant regardless of changes in load torque. The superposition of the load torque of the electromagnetic torque of the machine and the evolution of the actual speed and estimated shows the proper monitoring of the load torque and two speeds (actual and estimated) are similar; implying the robustness and stability of the system because of fuzzy controller.
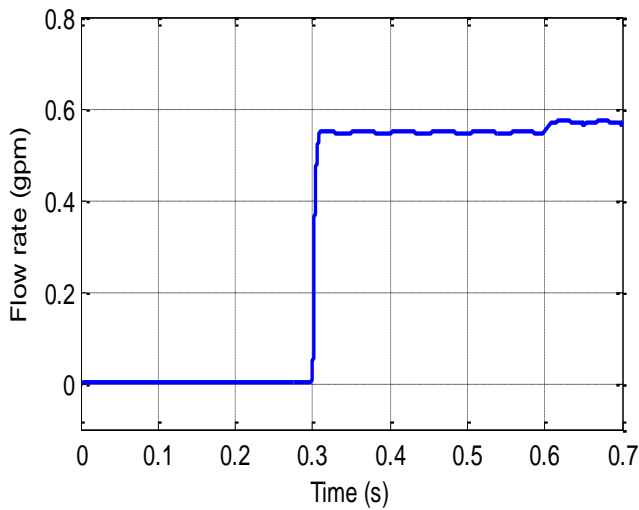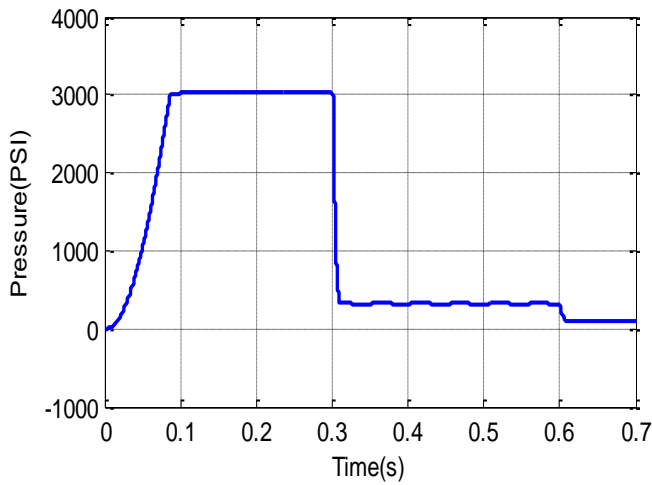
Fig. 11 Response torque and speed of IM with FLC
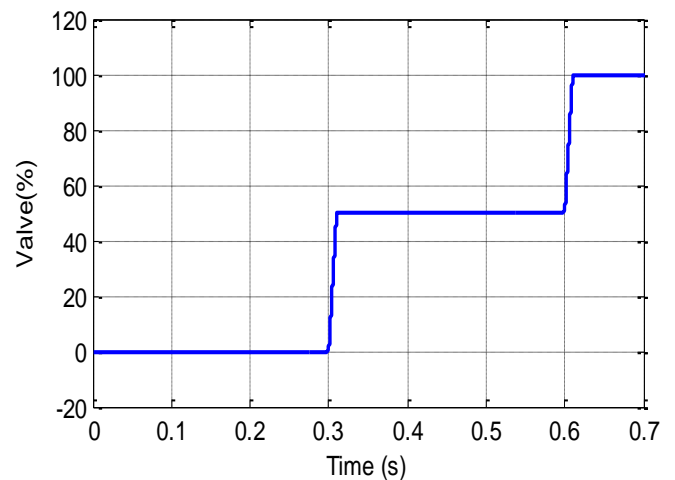


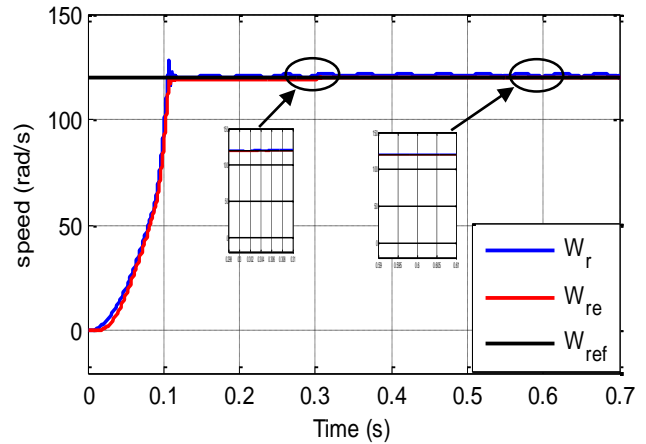Fig. 10 Response of valve, pressure and flow rate of pump


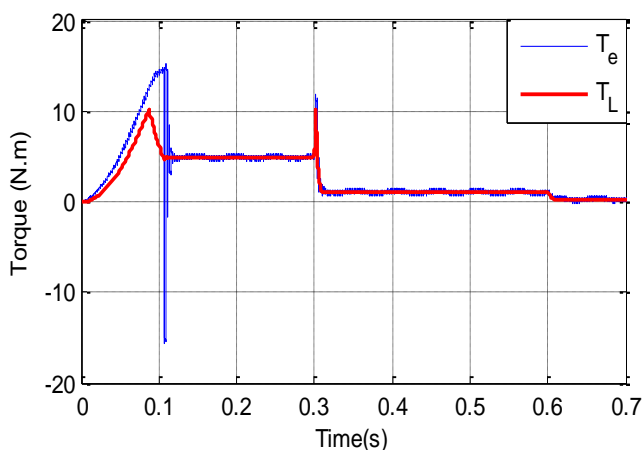
## VIII.   CONCLUSION

The paper presented the control sensorless speed of an induction motor of photovoltaic pumping system. Concerning the photovoltaic generator, a mathematical model (current-voltage) of the equivalent electrical circuit, taking into account temperature, allowed to estimate quickly and accurately the energy considered for weather conditions radiation and temperature. The PV energy conversion of describing the concept of modularity of the conversion chain, the development of new architectures with very high conversion efficiency. This maximization of production , given the fluctuating nature of the PV source considered and ensured through efficient MPPT control types , high yields, especially during sudden changes of sunshine . For our part, we opted for a control against voltage feedback.

The study results obtained show that the transitional regime is less oscillatory and a fast look back with a fuzzy controller, it ensures the best performances in response time and exceeding when starting and reversing direction of rotation, and sudden load changes are amortized, peak values of the speed are avoided.

### REFERENCES

[1]   B. Prabodh, D. Vaishalee, "Hybrid renewable energy systems for power generation in standalone applications". *Renewable and Sustainable Energy Rev*, vol 16 no. 5, pp. 2926-2939, 2012.

[2]   A. Chaouachi, M.K. Rashad, K. Nagasaka, "A novel multi-model neuro-fuzzy-based MPPT for three-phase grid-connected photovoltaic system". *Solar Energy*. vol. 84, no. 12, pp. 2219-2229, December 2010.

[3]   L. Shuhui, A.H. Timothy, L. Dawen, H. Fei, "Integrating photovoltaic and power converter characteristics for energy extraction study of solar PV systems". *Renewable Energy*.vol. 36, no. 12, pp.3238-3245, 2011.

[4] Y. Himri, AS. Malik, A. BoudgheneStambouli, S. Himri, B. Draoui, "Review and use of the Algerian renewable energy for sustainable development". *Renewable and Sustain Energy Reviews*. vol. 36, pp. 1584-1591, 2009.

[5] R. Faranda, S. Leva, "Energy comparison of MPPT techniques for PV Systems". *WSEAS Transcations on Power Systems*, pp. 1-6,2008.

[6] A. Mellit, A.K. Soteris, "Artificial intelligence techniques for photovoltaic applications". *Elsevier -Progress in Energy and Combustion Science*. vol. 36, no. 5, pp. 574-632, October 2008.

[7] A. Kalirasu, S. SekarDash, "Simulation of Closed Loop Controlled Boost Converter for Solar Installation".*Serbian Journal of Electrical Engineering*.vol. 7, no. 1, pp, 121-130,2010.

[8] N. Mohan, T.M. Undeland, W.P. Robbins, "Power Electronics, Converters Applications and Design". *John Wiley& Sons*, Inc, 1995.

[9] A. Nasri, A. Hazzab, I. Bousserhane, S. Hadjeri, P. Si-card, "Two Wheel Speed Robust Sliding Mode Control for Electric Vehicle Drive". *Serbian Journal of Electrical Engineering*.vol. 5, no. 2, pp. 199-216 , 2008.

[10] M. Malinowski, " Sensorless Control Strategies for Three-Phase PWM Rectifiers", Ph.D. Thesis, *Warsaw University of Technology*, Warsaw, (2001).

[11] J. Ghafouri and al, "Dynamic Modeling of Variable Speed Centrifugal Pump Utilizing MATLAB / SIMULINK". *International Journal of Science and Engineering Investigations*. Vol. 1,no. 5.pp ,2012.

[12] N, Hamrouni, M. Jraid, A, Cherif, A, Dhouib, "Measurements and Simulation of a PV Pumping Systems Parameters Using MPPT and PWM ControlStrategies". *IEEE Melecon*.pp. 885-888, 2006.

[13] Yeu Wu, Biaobiao Zhang, Jiabin Lu, K.L Du, " FuzzyLogic and Neuro-Fuzzy System: A Systemetic Introduction", *International Journal of Artificial Intelligence and Expert Systems*,Vol. 2, N°. 2, 2011, pp 47-80.

[14] P. L. Jansen and R. D. Lorenz, "A physically insightful approach to the design and accuracy assessment of flux observers for field oriented IM drives," *IEEE Trans. Ind. Applicat.*, vol. 30, pp. 101–110, Jan/Feb. 1994.

[15] W. Parkc, H. Kwonw, "Simple and robust sensorless vector control of induction motor using stator current based MRAC".*Electric Power SystemsResearch*,vol. 71, no. 3, pp. 257-266, November 2004.

[16] K. Bimal, K. Bose, "An Adaptive Hysteresis-Band Current Control Technique of a Voltage-Fed PWM Inverter for Machine Drive System". *IEEE Tran on Industrial Electronics*. Vol. 37, no. 5.pp. 402-408,1990.

[17] F.Z. Peng, T. Andfukao, "Robust Speed Identification for Speed Sensorless Vector Control of Induction Motors". *IEEE Trans.Indus. Applica*.vol. 30, no. 5, pp. 1234-1240, 1994.